

Performance Monitoring of Rammed Aggregate Piers® (RAPs)

Ece Kurt Bal, M.Sc., Sentez Insaat, Istanbul, Turkey; email: ekurt@sentezinsaat.com.tr

Lale Oner, M.Sc., Sentez Insaat, Istanbul, Turkey; email: loner@sentezinsaat.com.tr

Kutay Ozaydin, Prof. Dr., Yildiz Technical University, Istanbul, Turkey; email: ozaydin.kutay@gmail.com

ABSTRACT: In this paper, settlement performance during water testing of structures at a wastewater treatment facility in Turkey, constructed on soils improved by the Rammed Aggregate Pier® (RAP) System, are presented. The soil profile is comprised of firm to stiff silty clay and medium dense silty sand of 10 m thickness, overlain on thick soft to medium stiff silty clay with thin inclusions of sand lenses. The main goals of the in-situ soil improvement, to eliminate the risk of liquefaction and to form a homogeneous crust to reduce the total and differential of settlements, were achieved by improving the soil with RAPs down to 15 m depth. To verify the design parameters, two kinds of field load tests, the modulus load test and areal loading test, were performed. Completed structures are water tested and settlements recorded, providing performance monitoring data under service loading conditions. With the implemented soil improvement, post construction settlements are reduced to 14-20 cm compared to the initially estimated 20-80 cm long term settlements, and differential settlements are reduced to permissible limits.

KEYWORDS: Impact rammed aggregate piers, stiffness, consolidation settlement, monitoring, ground improvement.

SITE LOCATION: [Geo-Database](#)

INTRODUCTION

The need of ground improvement methods has increased significantly in recent years due to the need for the construction of transportation, hydraulics, and industrial structures at unfavorable soil conditions. Among existing alternatives, the Rammed Aggregate Pier® (RAP) solution has been listed and served as an alternative to deep foundations or over excavation and replacement of compressible soils (Lawton et al., 1994). RAPs are mainly used to reduce intolerable settlements, mitigate the liquefaction potential, reinforce slopes, and improve the bearing capacity of footings, mat foundations, embankments, reinforced earth walls, transportation, and port structures, etc. in Turkey as a cost-effective solution for construction on soft/compressible soil layers. The RAP soil reinforcement system has been successfully applied to many sites with peat, highly organic soil, and very soft soil zones (Fox and Edil, 2001). In addition, it is expected that vibration and volumetric densification during the construction of RAPs provide an additional benefit to increase the strength and stiffness properties of cohesionless soils (sandy, gravelly, and relatively non-plastic silty material). The combination of RAP materials and the vertical ramming inherent in the RAP construction process results in a well-coupled pier-soil response that transfers shear stresses effectively across the soil-pier interface, whereby the response is a byproduct of the unique construction process (Wissmann et al., 2015).

Within the context of this manuscript, the settlement performance of structures at a wastewater treatment facility where foundation soils were improved with 50 cm diameter RAP Impact elements are assessed. The settlement of structures are analyzed with Settle 3D, a RocScience software program using the information from site soil investigation and compared with instrumentation data collected from a test embankment. The settlement behavior is further analyzed by comparing the estimated consolidation settlements and the recorded settlements during the water tests performed after the construction of structures. Before discussing the field load tests and their results, the installation methodology of RAPs along with the site soil profile will be explained.

Submitted: 2 August 2018; Published: 21 May 2020

Reference: Bal E.K., Oner L., and Ozaydin K. (2020). Performance Monitoring of Rammed Aggregate Piers® (RAPs). International Journal of Geoengineering Case Histories, Volume 6, Issue 1, pp. 37-52, doi: 10.4417/IJGCH-06-01-02

PROJECT DESCRIPTION AND SUBSURFACE CONDITIONS

The project site is located on the Marmara Sea coast at a flat topography, along the Yalova-Izmit Highway, between Yalova city center and the Topcular pier. The eastern sides and south and west sides of the site are surrounded by factories and some empty lots, respectively. The ground level is around sea level and the maximum elevation is +1.0 m. The project site for the wastewater treatment facility is shown in Figure 1. Excessive settlement of the structures, which are founded on shallow foundations, is a concern. The foundation pressures from these main structures are around 80-110 kPa. In addition to these main structures, auxiliary structures such as distribution tanks and ducts, pumping stations, and operational and administrative buildings which are all connected to each other have foundation pressures around 50-70 kPa. A schematic view of the facilities is shown in Figure 2.



Figure 1. Location of the site.

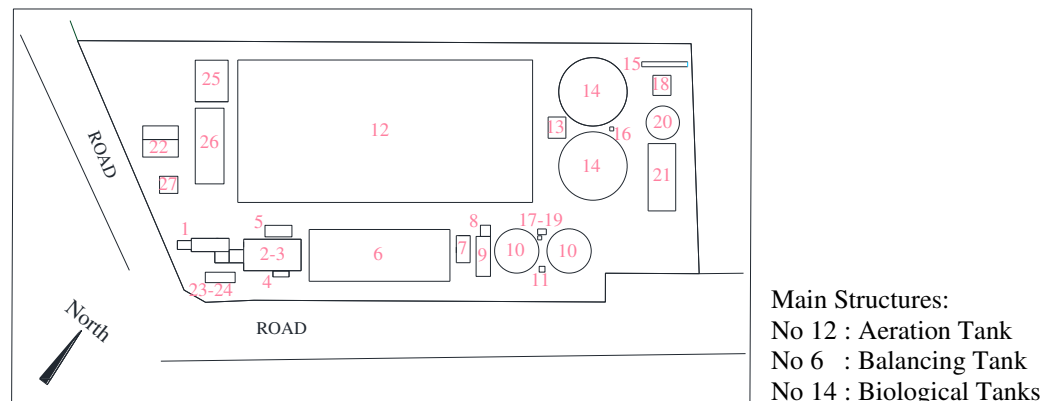


Figure 2. The layout plan of wastewater treatment facility.

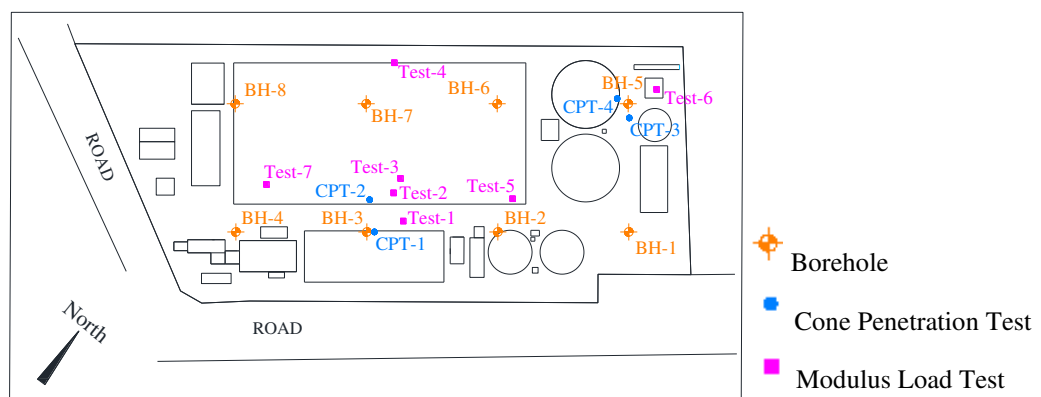


Figure 3. Boring, CPT, and modulus load test location plan.

A site investigation program, involving 25-35 m deep boreholes at 8 different locations and 20-26 m deep CPT soundings at 4 different locations were executed as shown in Figure 3. At various depths, standard penetration tests were performed along with the disturbed and undisturbed soil sampling. On the retrieved soil samples, soil classification, unconfined compression, and consolidation tests were conducted.

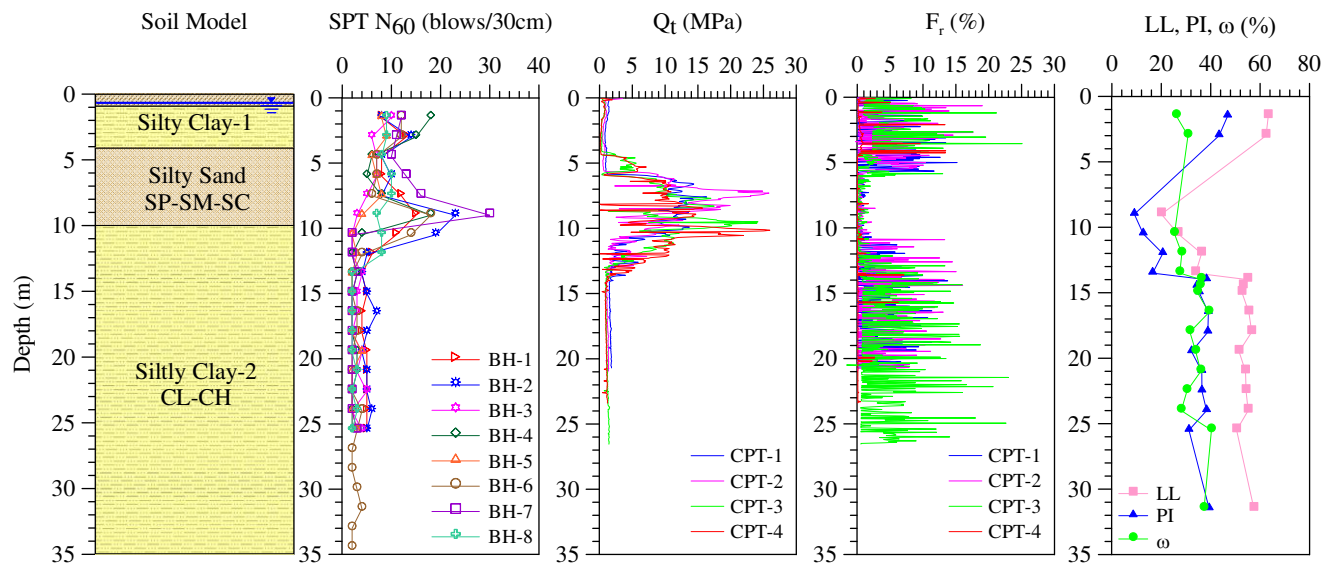


Figure 4. The representative soil profile, the variation of SPT N_{60} , Q_t , F_r , LL, PI, and ω with depth.

The representative soil model, together with variations with depth of corrected cone tip resistance (Q_t) and friction ratio (F_r) from cone penetration tests, SPT N_{60} values from standard penetration tests, liquid limit (LL), plasticity index (PI), and natural water content (ω) are shown in Figure 4. The soil profile includes a 0.2-1.0 m thick top soil layer overlying a medium stiff to stiff silty clay layer down to a depth of 4.0 m. Below this clay layer, a 6.0 m thick loose to medium dense silty sand layer is encountered, which overlies very thick soft to medium stiff silty clay layers with thin inclusions of loose to medium dense silty sand lenses. The ground water table is reported to be at 0.70 m below natural ground surface. Table 1 shows the summary of soil parameters.

Table 1. Summary of soil parameters.

Material	γ (kN/m ³)	ω (%)	LL (%)	PI (%)	c_u (kPa)	ϕ' (°)	E_s (MPa)
Silty Clay	18.0	27	63	47	50	21	7.5
Silty Sand	18.0	-	-	NP	-	30	25
Silty Clay-2	18.0	44	48	31	50	23	7.5

γ : Unit weight (Robertson and Cabal, 2010)

ω : Natural water content, average values of laboratory test results

LL : Liquid limit, average values of laboratory test results

PI : Plasticity index, average values of laboratory test results

c_u : Undrained shear strength, $c_u = (q_u - \sigma_v)/N_{kt} \rightarrow N_{kt} = 14$ (Robertson and Cabal, 2010) (for Silty Clay-1 layer); $c_u = q_u/2$ (for Silty Clay-2 layer)

ϕ : Effective friction angle, $\phi' = 39 - 11 \log PI$ for clay layers (Sorenson, 2013); $\phi' = 27.1 + 0.3N_{60} - 0.00054(N_{60})^2$ for sandy layers (Das, 2014)

E_s : Deformation modulus, $E_s = (3-8)q_c$ for soft clay, clayey silt (Bowles, 1996); $M = 1.7(q_c + 1.6)$ for clayey sand (Meigh, 1987)

GROUND IMPROVEMENT WITH RAMMED AGGREGATE PIERS (RAPs)

Design Consideration

At the preliminary design stage, the elastic and consolidation compression response of the site under loads to be imposed by the structures is assessed by using Settle 3D, RocScience software, which enabled 3D settlement analysis. The Settle 3D model used for the analyses is shown in Figure 5. In the calculations, a "flexible" foundation assumption is adopted to assess

the differential settlement potential of the site and Boussinesq stress distribution is adopted for the estimation of stress increase beneath loaded areas. In the consolidation settlement computation, for soft clay and medium stiff clay layers the compression index ratio is taken as of $C_c/1+e_0=0.12$ and $C_s/1+e_0=0.06$, respectively, and $OCR=1.0$. The consolidation settlements are estimated to vary in the range of 20-82 cm under the service loads, and their distribution is shown Figure 6.

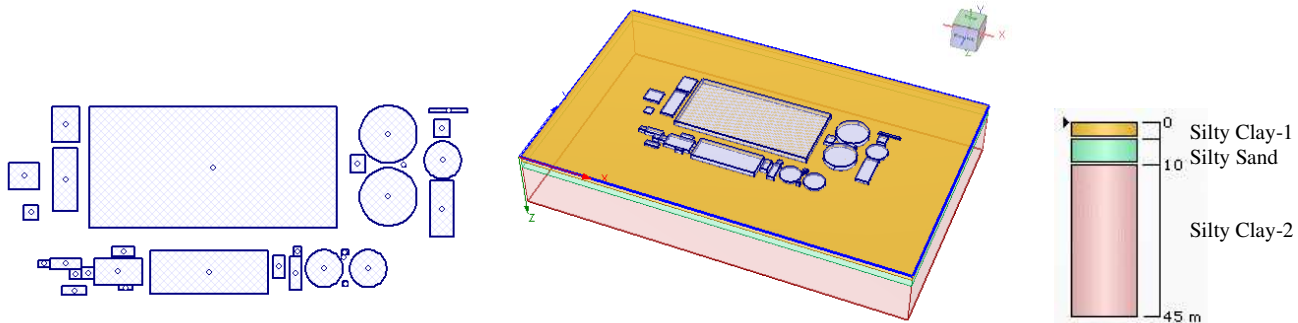


Figure 5. Settle 3D model.

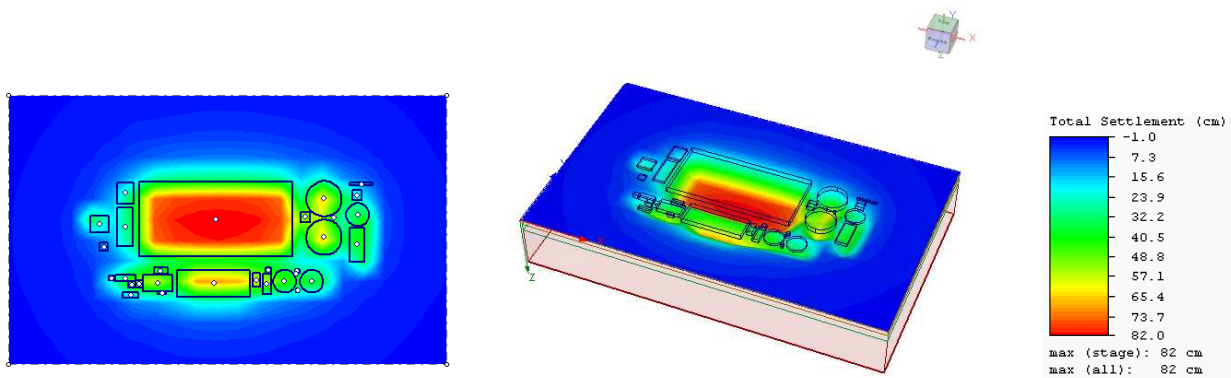


Figure 6. Estimated total settlement without improvement.

In order to eliminate liquefaction induced strength and rigidity losses of bearing layers under the foundations (the liquefaction triggering potential of silty sand layers) and to limit the excessive surface settlements, it is decided to implement a soil improvement solution. The total elimination of the settlements is considered to be a task not easily (or economically) achievable, and found to be not necessary for the proposed use of this site. Hence, the main goal of the in-situ soil improvement is defined as to form a thick homogeneous crust with improved soil properties under the foundations. The detrimental effects of the differential settlements reflected on the ground surface are expected to be minimized if a thick crust is located at the top of the soil profile. After a careful review of soil improvement methods which are available and can be implemented at the site to achieve the goals set, the use of Rammed Aggregate Pier® (RAPs) is preferred.

Assessment of Liquefaction Susceptibility

Liquefaction potential was identified according to SPT N values and laboratory test results for the silty sand layers with a thickness of 6 m under a design earthquake motion of maximum acceleration $a_{max}=0.40$ g and moment magnitude $M_w=7.5$. The silty sand layer with varying fines content (10% to 40%, typically 20%) is predicted to liquefy ($FS= 0.18-0.88$) by using the approaches for Cyclic Stress Ratio (CSR) and Cyclic Resistance Ratio (CRR) calculations proposed by Seed and Idriss, 1971, and Youd and Idriss, 2001, respectively, if mitigative ground improvement is not applied. RAPs can be used to mitigate the liquefaction potential of sandy soils by densifying the soils surrounding the installed RAP elements. The vibratory vertical ramming during the installation of RAPs in a loose, saturated sand deposit can potentially mitigate the risk of liquefaction by decreasing the seismic demand on the soil by redistributing the induced shear stress from the sand to the high modulus rammed aggregate piers (Farrell et al., 2010). The design CSR is estimated using the shear stress reduction factor, S_R , using

the equation below which is based on shear strain compatibility assumption (Baez and Martin, 1995) even though the validity of this assumption is questioned by many researchers for columns of high rigidity.

$$S_R = \frac{1}{G_r} \times \frac{1}{R_a + \frac{1}{G_r}(1-R_a)} \quad (1)$$

where, $R_a = A_{RAP}/A$, $G_r = G_{RAP}/G_s$, A_{RAP} =area of RAP elements, A =cell area, G_{RAP} =shear modulus of RAP elements, and G_s =shear modulus of matrix soil. As shown in Figure 7a, the factor of safety against liquefaction after improvement was obtained higher than 1.0 by using the design CSR ($= CSR \times S_R$). It is assumed that the additional benefit in the sandy layers is obtained by vibration and volumetric densification during the construction of RAPs, which increases the SPT values in the order of 5-8 blows/30cm compared with pre-improvement values according to densification guidelines for RAP Impact elements in sands (Zeng, 2010).

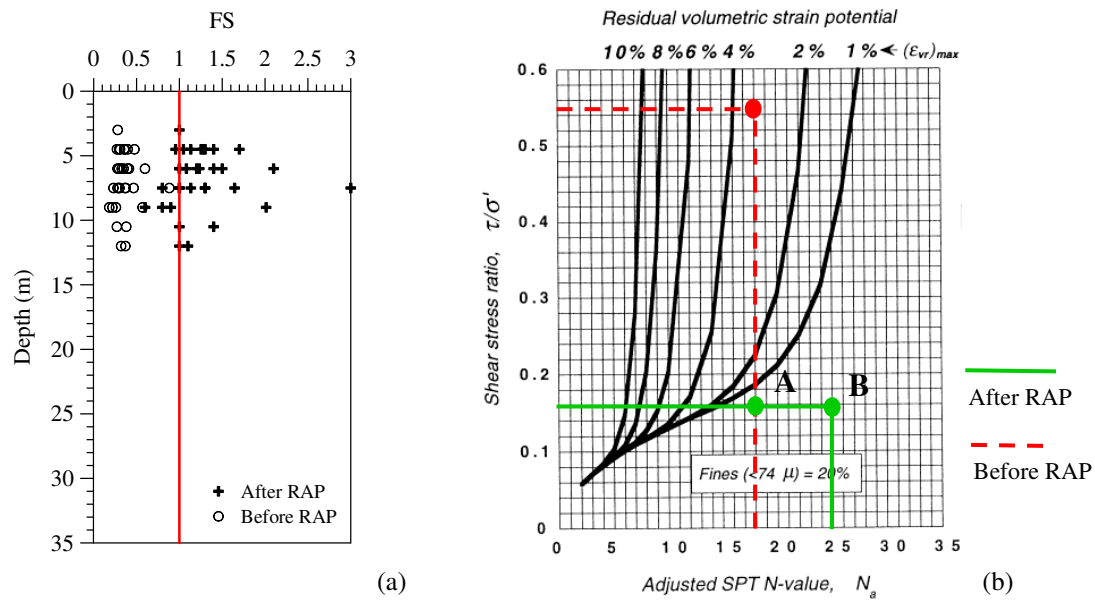


Figure 7. a) Liquefaction susceptibility of silty sand layer before and after RAP applications; b) Relationship between normalized SPT N value and shear strain potential for the case of $FC=20\%$ (Shamoto et al., 1998).

Also, the Shamoto et al. (1998) chart given in Figure 7b is used for the prediction of residual volumetric strain potential. The individual volumetric strain values of each-sub-layer are first estimated by using the chart and summed up to obtain the total ground settlement. After the installation of RAP elements, the post liquefaction settlement of the cohesionless soil layer of 6 m thickness, which is estimated as 19 cm before improvement, is reduced to 3 cm due to shear stress ratio reduction according to Equation 1 (Point A). It is observed from Figure 7b that even if the SPT N value increase due to densification for the sandy layers between the columns is ignored (Point B), the volumetric strain potential is below 1% after the ground improvement.

Construction of RAP Impact Elements

Installation steps for these stone columns with the displacement technique are summarized below:

1. A closed-ended mandrel with a diameter of 36 cm is pushed into the design depth using hydraulically induced static force assisted with vertical dynamic energy,
2. The mandrel and hopper are filled with aggregate (typically graded 13 to 38 mm particle size), and
3. The ramming action is applied with 100 cm up / 67 cm down compaction efforts, during which vertical dynamic energy is also introduced.

The ramming action expands the diameter from 36 cm to 50 cm when the 100 cm up / 67 cm down compaction procedure is chosen. The significant increase in lateral stress, combined with the high density of the stone created by this installation process, provides the unique strength and stiffness of the RAP system (Handy, 2001; Wissmann et al., 2001). Figure 8 presents the construction methodology of RAP Impact elements and a view from the field construction.



Figure 8. Construction methodology of RAP Impact elements and a view from the field construction.

Design Approach

In order to achieve the design goals, 50 cm diameter, very stiff RAP elements reaching to 15 m length from the ground surface with 1.4 to 1.7 m square pattern, corresponding to area replacement ratios of 10% and 7% respectively, were installed beneath the main structures of the wastewater treatment facility. The closest spacing was used beneath the aeration tank mat with the highest base pressure of 110 kPa.

Foundation settlements are calculated using a two-step procedure: the compression of the zone of matrix soil reinforced by the piers (upper zone) is first estimated, and then the compression of the zone of soil that is located below the tip of the piers (lower zone) is computed. The sum of the two yields the total settlement.

The compression of the RAP-reinforced zone beneath the mat is estimated by using composite constrained modulus of improved soil, E_{comp} . The representative values of E_{comp} for the upper zone layers are computed by considering the area ratios of RAP and properties of natural soil and piers. The composite constrained modulus for a RAP improved soil zone is computed using the following relationship (Poulos, 1993):

$$E_{comp} = E_{RAP} R_a + E_s (1 - R_a) \quad (2)$$

where E_{RAP} is the compression modulus of RAPs, E_s is the constrained modulus of matrix soil, and R_a is the area replacement ratio. The area replacement ratio for a square pattern of RAPs, R_a , can be expressed in terms of the diameter and spacing of the piers as follows:

$$R_a = \frac{A_{RAP}}{(s_p)^2} \quad (3)$$

where A_{RAP} is the area of the compacted piers (0.2 m^2 for diameter of 50 cm) and s_p is the center to center spacing of piers. Estimates of settlement in the lower zone materials, below the bottom of the pier bulbs, are computed using conventional geotechnical settlement analysis procedures.

Settle 3D analyses are carried out for the improved soil conditions, considering the presence of RAPs of 15 m length under the foundation base. Elastic settlements are calculated for the upper zone (i.e., in the improved upper 15 m) with an assumed RAP stiffness modulus value of 25 MN/m^3 , and consolidation settlements of the lower zone are calculated using properties of underlying layers. Soil parameters used in upper zone settlement analyses are shown in Table 2. The estimated total settlement before and after improvements is shown in Table 3 comparatively.

Table 2. Soil parameters used in upper zone settlement analyses.

Depth (m)	Material	RAP Zones	γ_{comp} (kN/m ³)	E_{RAP} (MPa)	E_{comp} (MPa)
0.0 – 4.0	Silty Clay-1	RAP Zone-1	18.4	50	12
4.0 – 10.0	Silty Sand	RAP Zone-2	18.4	100	32
10.0 – 15.0	Silty Clay-2	RAP Zone-3	18.4	50	12

Table 3. The estimated total settlement before and after improvement (preliminary design).

No	Unit	q_{max} (kPa)	RAP Spacing (mm)	RAP Length (m)	Total Settlement (cm)			
					Before Improvement		After Improvement	
			$\sum S_{\text{center}}$	$\sum S_{\text{edge}}$	$\sum S_{\text{center}}$	$\sum S_{\text{edge}}$		
T01	Preliminary Treatment Unit	80	1.7 x 1.7	15	40.6	25.2	6.6	4.7
T02-03	Preliminary Treatment Unit	80	1.7 x 1.7	15	56.9	36.6	15.0	10.8
T04	Preliminary Treatment Unit	80	1.7 x 1.7	15	49.7	35.5	12.0	9.8
T05	Sand on Oil Holder Building	50	1.7 x 1.7	15	49.8	35.7	14.7	12.8
T06	Balancing Tank	100	1.4 x 1.4	15	68.6	57.0	21.4	17.3
T07	Balancing Tank Pump Station	100	1.7 x 1.7	15	60.3	48.2	16.5	16.0
T08	Chemical Treatment Unit	80	1.7 x 1.7	15	53.5	41.4	14.9	14.3
T09	Chemical Treatment Unit	80	1.7 x 1.7	15	54.0	33.7	13.8	9.5
T10-1	Chemical Sedimentation Tank	50	1.7 x 1.7	15	46.5	38.5	11.6	12.4
T10-2	Chemical Sedimentation Tank	50	1.7 x 1.7	15	43.0	33.5	9.3	9.3
T11	Distribution Tank-1	100	1.7 x 1.7	15	40.9	29.7	8.2	6.9
T12	Aeration Tank	110	1.4 x 1.4	15	81.4	55.1	30.1	13.8
T13	Distribution Tank -2	80	1.6 x 1.6	15	59.6	45.3	17.9	16.4
T14-1	Biological Tank	100	1.5 x 1.5	15	65.4	46.8	19.0	11.5
T14-2	Biological Tank	100	1.5 x 1.5	15	66.1	57.3	19.5	17.6
T15	Flow Meter	30	1.6 x 1.6	15	25.7	13.7	4.9	2.8
T16	Biological Sed. Pump Chamber	80	1.6 x 1.6	15	49.2	41.7	14.9	14.0
T17-19	Chemical Sed. Pump Chamber	80	1.7 x 1.7	15	44.2	33.1	10.7	9.7
T18	Return Sludge Pump Station	70	1.6 x 1.6	15	44.5	26.6	8.7	5.7
T20	Sludge Tank	50	1.6 x 1.6	15	44.3	29.8	10.2	6.9
T21	Chemical and Sludge Dewatering	60	1.6 x 1.6	15	46.2	23.7	10.2	4.9
T22	Operation Building	50	1.7 x 1.7	15	40.2	21.3	7.6	4.4
T23-24	Servis Water Storage and Pump St.	50	1.7 x 1.7	15	37.2	21.3	7.1	4.6
T25	Substation	40	1.6 x 1.6	15	41.6	21.1	10.1	5.3
T26	Blower Tank	50	1.6 x 1.6	15	48.1	26.4	12.8	7.5
T27	Guard Building	20	1.7 x 1.7	15	25.0	14.0	5.1	3.8

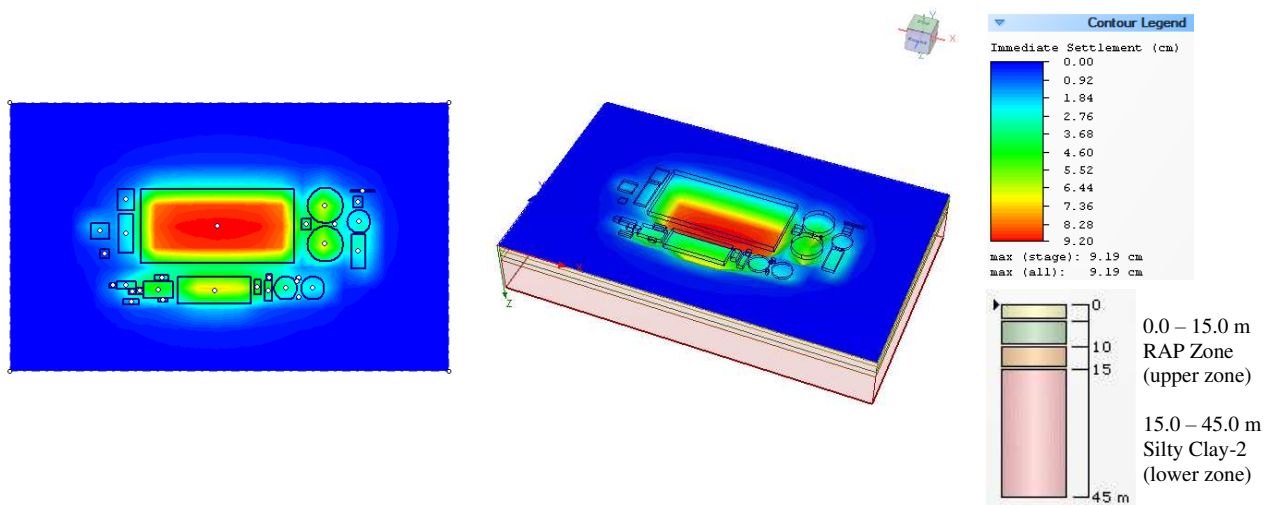


Figure 9. Upper zone settlement (improved zone).

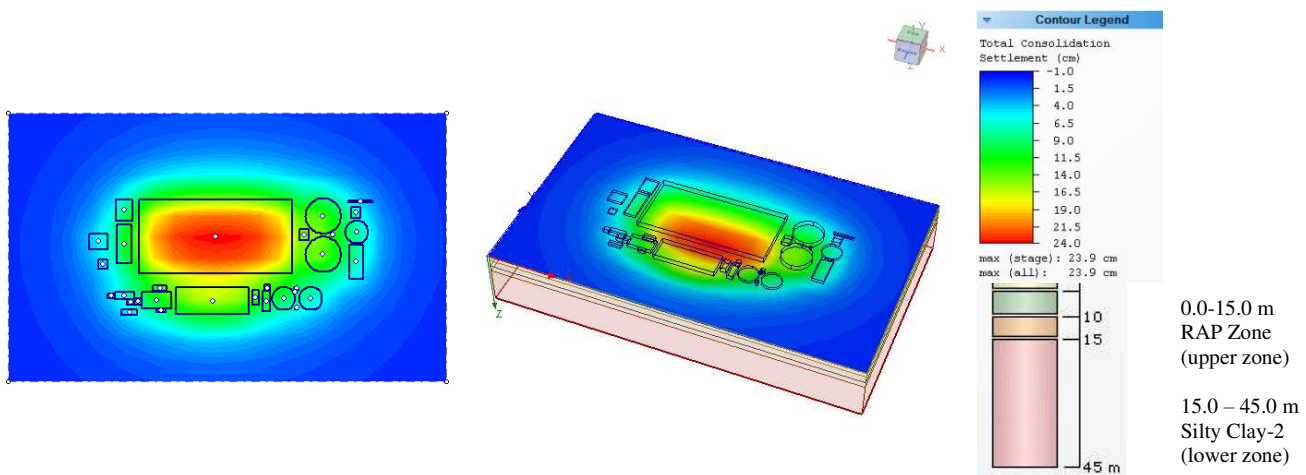


Figure 10. Lower zone settlement (unimproved zone).

At the preliminary design stage, the immediate settlement of the improved upper layers with RAP elements and the long term consolidation settlement of non-improved cohesive layers underlying RAP elements were computed to be in the range of 10 cm and 14-20 cm, respectively, indicating a considerable decrease in total settlements compared to the consolidation settlements estimated to be in the order of 20-82 cm if no soil improvement with Impact RAPs is implemented. The distribution of computed settlements shown in Figures 9 and 10 indicates that a considerable decrease in differential settlements can be expected with the planned soil improvement.

Modulus Load Test Procedures and Results

An assumed pier modulus value is selected using methods described in literature (Lawton and Fox, 1994) based on known pier properties and the properties of the surrounding soil, and then confirmed with site specific modulus tests. These tests are widely known as "quick" tests due to relatively rapid application of the loading scheme. The test set-up is similar to a pile load test configuration and the test is performed in general accordance with ASTM D-1143. The tests are also used to observe how the RAP behaves in the soil matrix by monitoring the deflection of tell-tales installed at the tip of the test piers. The modulus load test of RAPs may also incorporate tell-tales at different elevations within the pier (Brian et al., 2006). The tell-tale elements consist of a horizontal steel plate that is attached to two sleeved vertical bars extending to the top of the pier. When a RAP is equipped with a tell-tale reference plate, the deformation mode of the pier can be recognized from the shape of the tell-tale load settlement curve in comparison with the top of the pier settlement. Typical modes of deformation for RAPs installed in soft soil include bulging and tip movement (Wissmann et al., 2002).

In this project, 7 modulus load tests were performed on RAPs installed with lengths of 14-16 m to assess the load bearing capacity and stiffness response of individual RAPs. As the axial compressive load was directly applied on the pier, the magnitude of stress was controlled by a hydraulic jack with a calibrated manometer. The construction machine was used as a counter weight for the modulus load tests performed in this project. The vertical displacements of the piers were monitored using five comparators which were connected to the transverse beam, and two of these comparators were placed on the tell-tale to measure the deformation at the bottom of piers. The distance of the bearing points of the transverse beam from the test pier was provided to be at 5 pier diameters. A concrete cap with a diameter of 60 cm was placed on top of the pier to transfer the load. A schematic drawing of the test set-up and the photos taken from the test area are shown in Figure 11.

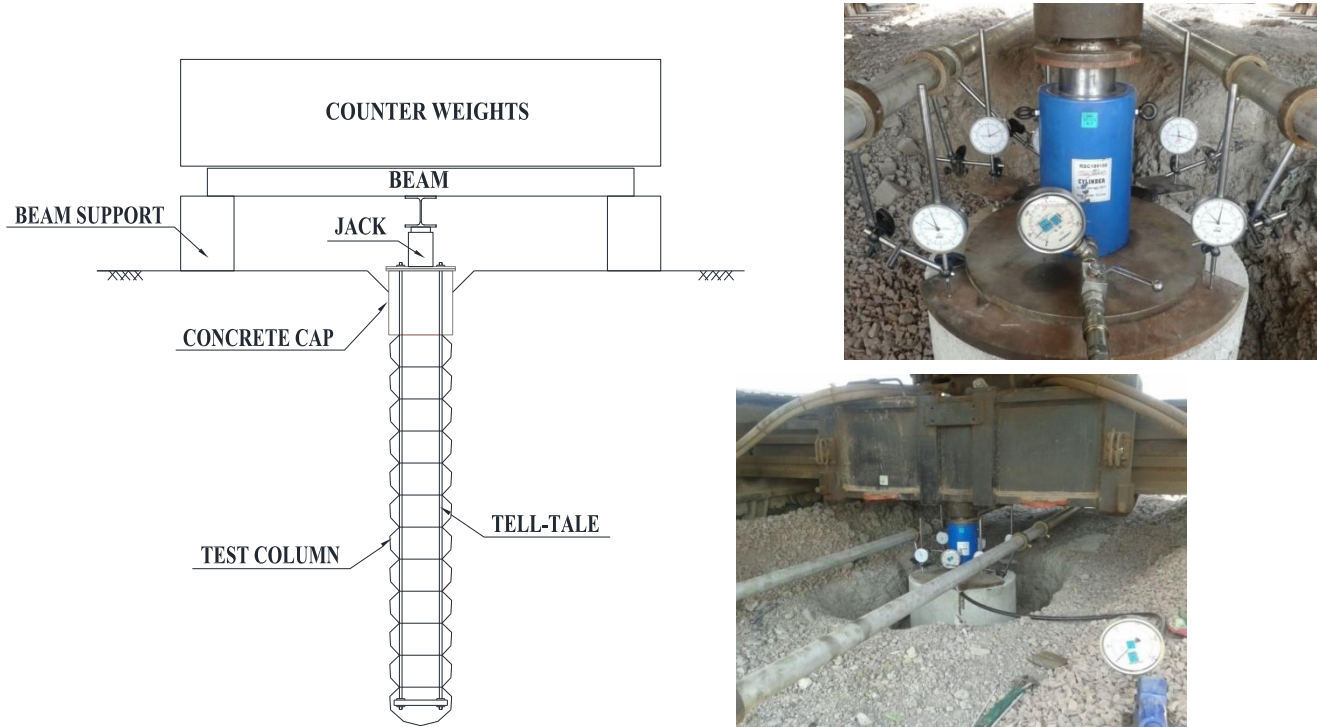


Figure 11. The test set-up and field photos.

Loading, starting with 5% of service load, was increased until the pier was tested up to the capacity of 150% of its service load. This was followed by an unloading procedure. All load increments were held for a minimum of 15 minutes and until the rate of deflection reduces to 0.254 mm per hour or less, or for a maximum duration of 1 hour. The load increment that represents approximately 115% of the design maximum stress on the Rammed Aggregate Pier was held for a minimum of 60 minutes and until the rate of deflection was less than 0.254 mm per hour or less, or for a maximum duration of 4 hours. Field load tests were performed by closely following the loading scheme summarized in Table 4.

Table 4. The loading scheme.

Load No	% Service Load	Load (ton)	Time (min. / max.)	Load No	% Service Load	Load (ton)	Time (min. / max.)
0	5	0.68	15/60	8	133	17.96	15/60
1	16	2.16	15/60	9	150	20.25	15/60
2	33	4.46	15/60	10	100	13.50	N/A
3	50	6.75	15/60	11	66	8.91	N/A
4	66	8.91	15/60	12	33	4.46	N/A
5	83	11.21	15/60	13	0	0.00	N/A
6	100	13.50	15/60	14	100	13.50	N/A
7	116	15.66	60/240	15	0	0.00	N/A

The load vs. settlement curves for test 5 and test 6 are shown in Figure 12a and Figure 12b, respectively. These tests were performed on a single pier extending to 16 m below grade. RAPs undergoing primarily elastic deformation with little tell-tale movement indicated sufficient mobilization of shaft friction, without bulging, to resist the applied stress. At design loads (13.5 ton), the deflection at the top of the test piers in all tests was measured in the range of 12 mm and 18 mm. The pier stiffness was determined from the slope of a plot of top-of-pier stress vs. top-of-pier deflection. The results indicated that a RAP stiffness of 35-70 MN/m³ can be adopted and showed that the stiffness value used in the preliminary design was on the safe side.

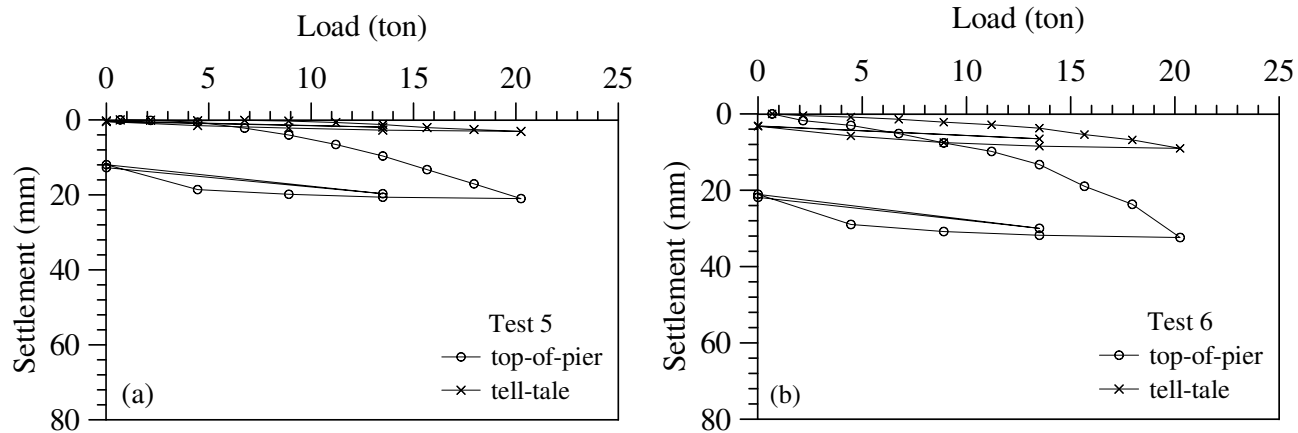


Figure 12. Modulus load tests, load-settlement graphs.

TEST EMBANKMENT AND ASSESSMENT OF MONITORING RESULTS

To verify the general design of soil improvement with the use of RAP elements and to determine the likelihood of differential settlements, a full scale area load test was performed by using a test embankment with 1V:1.5H side slopes, 6.1 m height and 36.8 m x 36.8 m base in plan. Test embankment was located at an area where soil conditions were relatively unfavorable as suggested by the boreholes. The area test contained 729 RAP elements of 15 m length and installed in a square grid with 1.4 m center to center spacing. The height and dimensions of the embankment were chosen to simulate the loading conditions expected in the project. A general view of test embankment is shown in Figure 13. Vertical deformations of the test embankment were monitored by geodetic measurements at 9 points (SP) for a period of 52 days. Also, a vibrating wire piezometer (transducers at 22.5 m and 27.5m depths) and four inclinometers installed to the depth of 40 m located outside of the test embankment were used for monitoring excess pore pressures and lateral deformations, respectively. Pore pressure transducers and inclinometers were monitored continuously during the construction of the test embankment, and then measurements were continued on weekly basis. The layout plan and the section of the load test embankment as well as the field photos are shown in Figures 14 and 15, respectively.

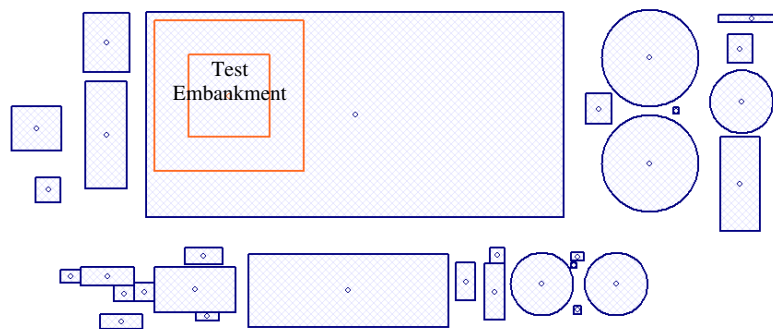


Figure 13. General view of test embankment.

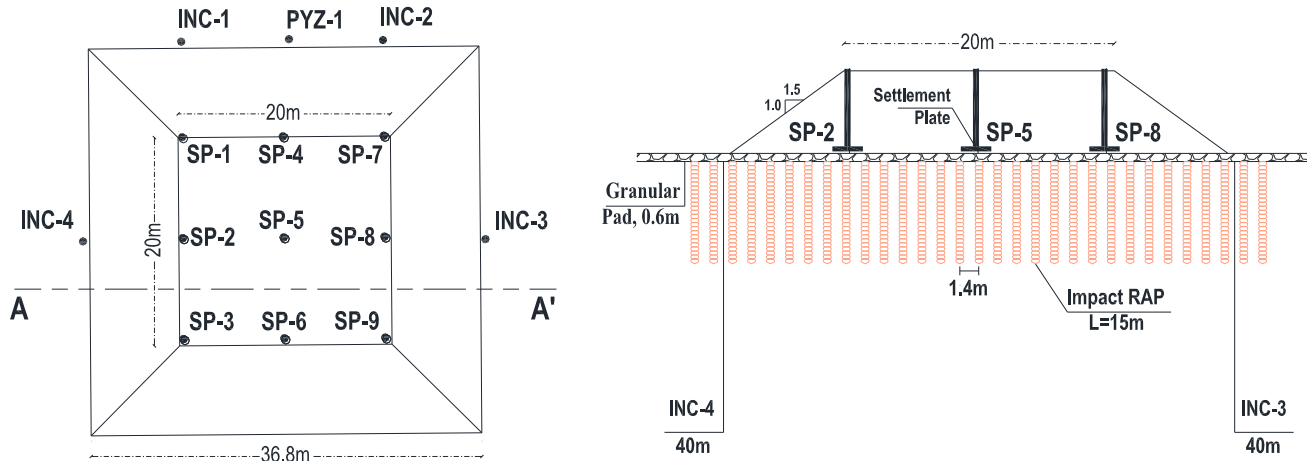


Figure 14. The layout plan and the section of test embankment.



Figure 15. The test embankment field photos.

Figure 16 shows settlement and pore water pressure-time response under the test embankment constructed on RAP improved ground. The geodetic measurements at 9 points (SP) for a period of 52 days indicated that the maximum settlements reached are around 28 cm or less, large portion of it occurring during construction. The piezometer measurements at depths of 22.5 m and 27.5 m indicated the initial readings of 236 kPa and 273 kPa, close to hydrostatic pressures of 225 kPa and 275 kPa, respectively, as shown in Figure 16. The piezometer measurements increased minimally (to 250 kPa and 283 kPa, respectively) during the embankment placement (probably due to radial drainage provided by the closely spaced RAP elements) and then decreased at a low rate toward their initial values. The four inclinometer readings installed around the test embankment showed the development of lateral displacement up to 90 mm during construction due to the rapid rate of fill placement (reaching maximum height in 7 days) and then movements slowed down after the full load of the embankment was imposed.

It can be assumed that the immediate settlements were completed during the construction of the embankment to its full height. The lower zone consolidation settlements expected to occur in all structures under service loads were computed using Settle 3D software and utilizing the estimated soil parameters from back analysis of observed behavior at the field load test.

In the consolidation settlement analysis for unimproved soil conditions, for the lower medium stiff silty clay layer, the compression index ratio was taken as $C_c/1+e_0=0.06$ ($C_c = 0.125$, $e_0 = 0.85$) and $OCR=1.0$. After soil improvement extending down to 15 m depth, only the lower silty clay layer is expected to contribute to consolidation settlements. On the other hand, because the wastewater treatment structures will cover very large areas, under service loads the stress increases in foundation layers will extend to greater depths than under the load testing conditions. Therefore, in the consolidation settlement analysis after soil improvement, unimproved lower silty clay layer was divided into two sub layers as silty clay 1/2 (15-45m depth) and silty clay-2/2 (45 to 75 m depth), and the soil parameters given in Table 5 were estimated from the back analysis of observed settlement behavior during the field load test shown in Figure 16.

It should also be noted that the dimensions of the loaded area and the rate of loading will affect the validity of one dimensional compression assumption used in the Settle 3D software. The soil parameters estimated by the back analysis from the load test settlement observations, which most likely included lateral displacements, are considered to be on the safe side.

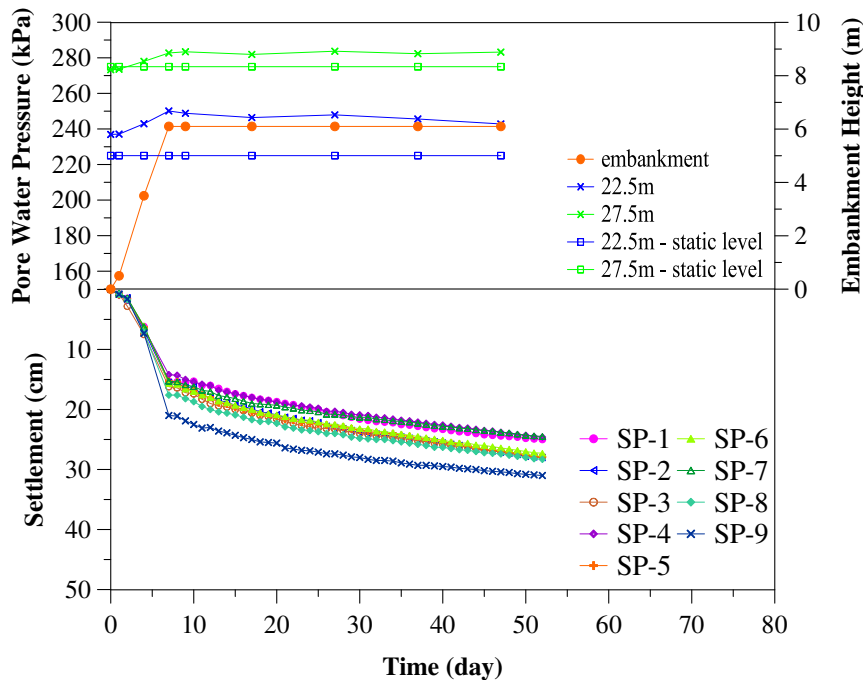


Figure 16. The measured results for the test embankment and instrumentation.

Table 5. Soil parameters use in Settle 3D assessments (after test embankment observations).

Material	Depth (m)	γ (kN/m ³)	$E_{comp.}$ (MPa)	C_c	C_r	e_0	$C_c/1+e_0$	$C_r/1+e_0$	OCR	c_v (m ² /day)
RAP Zone-1	0.0 – 4.0	18.4	12	-	-	-	-	-	-	-
RAP Zone-2	4.0 – 10	18.4	32	-	-	-	-	-	-	-
RAP Zone-3	10 – 15	18.4	12	-	-	-	-	-	-	-
Silty Clay-1/2	15 – 45	18.0	-	0.270	0.054	1.10	0.12	0.025	1	0.03
Silty Clay-2/2	45 – 75	18.0	-	0.125	0.025	0.85	0.06	0.013	2	0.03

Figure 17 shows the distribution of the estimated settlements arising from the consolidation of the unimproved lower zone. Consolidation settlements in the range of 7-45 cm can be expected when all structures are constructed and fully loaded. The excess pore pressure measurements taken during the load test (Figure 16) and vertical distribution of computed settlements from the Settle 3D analysis (Figure 17) indicate that layers down to 22 m depth are expected to contribute considerably to the consolidation settlements. In addition, it is expected that the settlements which will take place under rigid mat foundations will be less than calculated since the flexible mat behavior is taken into account in the analyses.

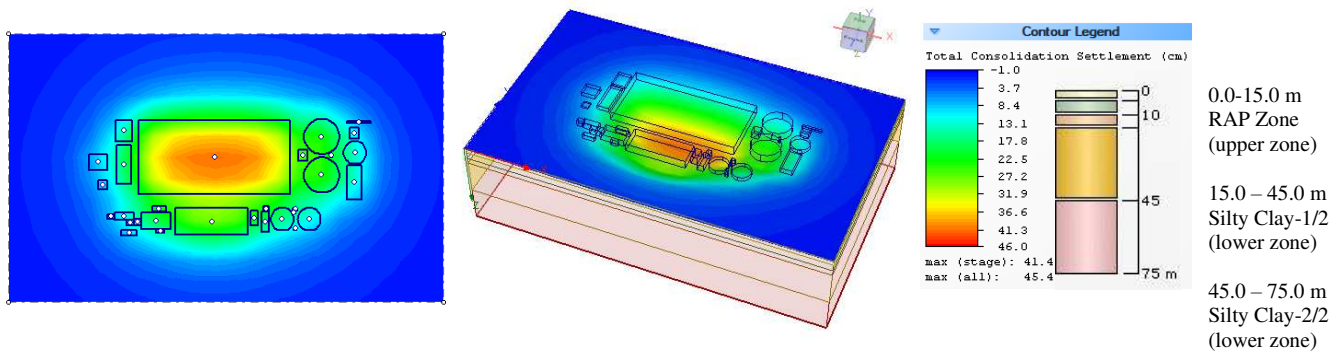


Figure 17. The consolidation settlements in the case of all structures constructed.

ASSESSMENT OF WATER TEST RESULTS

The construction of the wastewater treatment facility structures supported by RAP elements was completed within approximately 6 months. Water loading tests are carried out to check the construction performance in such facilities. During the water loading tests within the scope of this project, the settlement measurements were taken for 302 days. The water height-time relationship applied in water loading tests is shown in Figure 18. In Figure 19, the measurement points are shown for the aeration tank, balancing tank, and biologic tanks. In Figure 20, the estimated settlement-time response using Settle 3D software is shown together with the settlement readings taken during the water loadings tests.

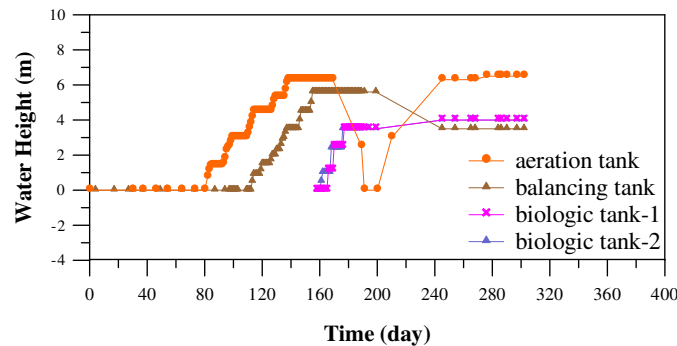


Figure 18. Water height–time relation applied in water loading test.

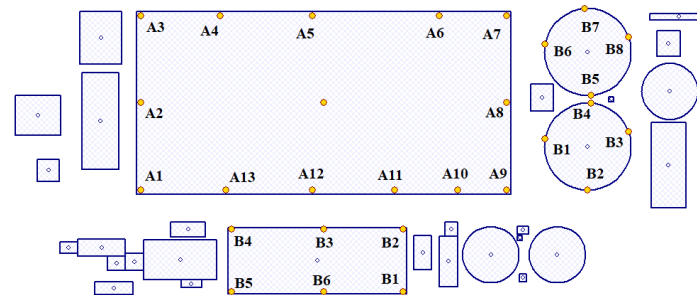


Figure 19. The measurement points for water loading test.

It is observed that under service loads of 96-108 kPa, in about 5.5 months after reaching the maximum of water level, the measured settlements reached values varying between 14.5 cm and 24 cm for the aeration tank, and 9.6 cm and 14.6 cm for the balancing tank. It was also observed that the settlements reached around 16 cm within 4 months under pressures of about 75 kPa for the biologic tanks. The total settlements recorded in the monitoring period were observed to be smaller than the average settlement values predicted by the 3D settlement calculations. This shows that the soil parameters estimated by back calculation from observed settlement behavior during the field load test were on the safe side, which may be attributed to the difference in the extent of influence zone and corresponding variations in soil conditions. As aforementioned, the loaded area in the field loading test was smaller compared to the dimensions of the structures water tested (especially more pronounced for the aeration tank), and the construction rate of the embankment for the field load test (6.1 m height reached in a week) was much faster than the loading rate in water tests. Therefore, while the one dimensional compression assumption was much more valid during the water testing of structures, its validity was plausible for the field load test, as indicated by up to 90 mm lateral displacements measured by the inclinometers.

It was also observed from settlement-time curves that the settlements were almost completed during the monitoring period, and the rate of settlements were quite consistent with the predictions based on the test embankment behavior. The distribution of measured final settlements on the plan is shown in Figure 21, and it is evident that the differential settlements are controlled to remain between 0.015 % and 0.25 % in accordance with the limiting values adopted among the project targets.

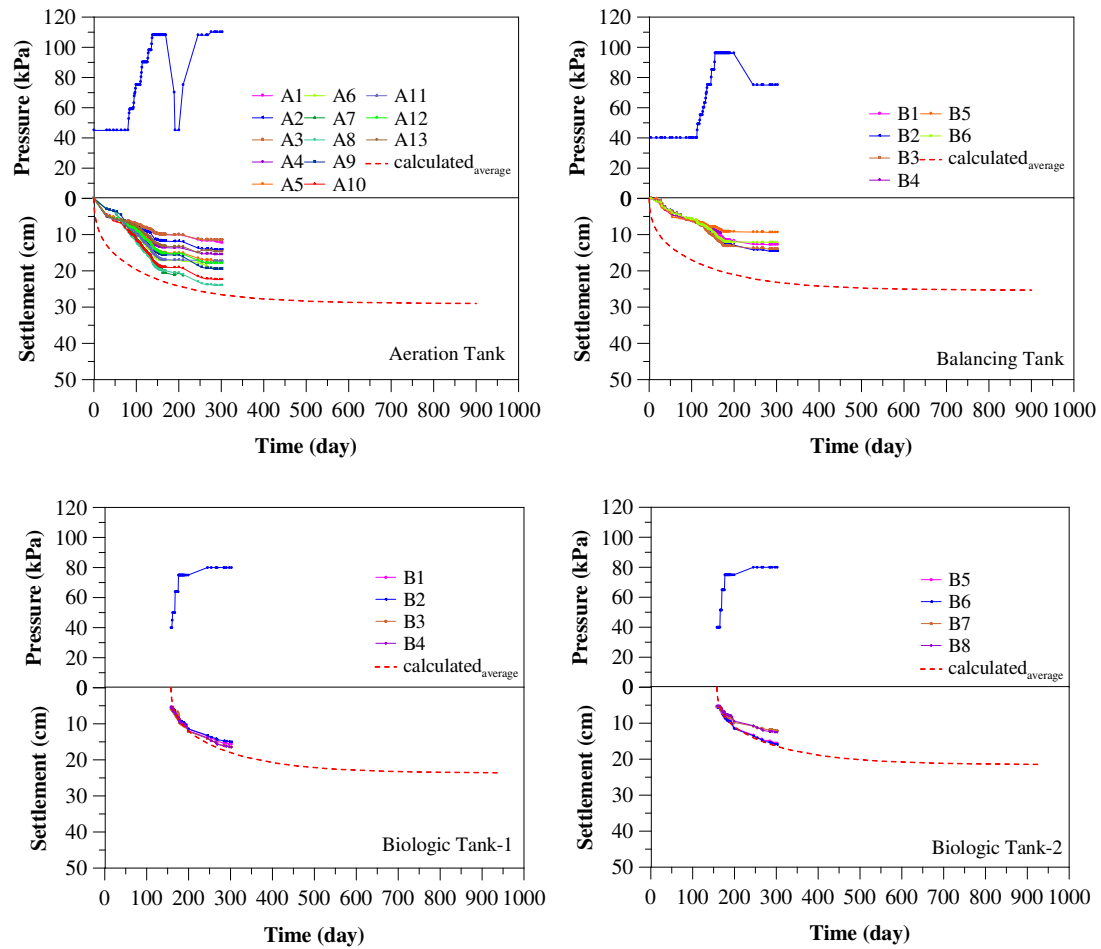


Figure 20. 3D model and field data responses: settlement vs. time curves for aeration, balancing, and biologic tanks.

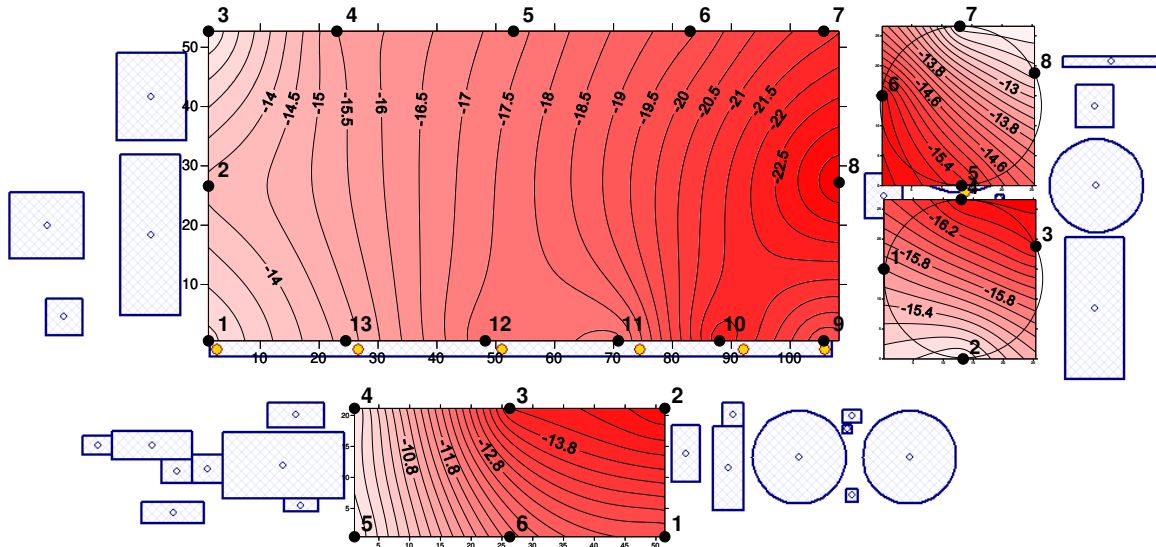


Figure 21. The distribution of measured final settlements on the plan.



CONCLUSIONS

This paper presents the results of settlement monitoring data at a wastewater treatment plant constructed on a soft clay site and reinforced with Rammed Aggregate Pier® elements (RAPs). Design goals in the implemented soil improvement scheme were: to reduce total and differential settlements; and eliminate liquefaction induced strength and rigidity losses of bearing layers under structures, as well as the detrimental effects of the differential settlements reflected on the ground surface during an earthquake by forming a thick strong crust on top of the soil profile. After the careful review of soil improvement methods available and determining what could be implemented at the site to achieve our goals, the use of the Rammed Aggregate Pier® (RAPs) was preferred.

In order to verify design assumptions, 7 modulus load tests were performed on 14-16 m long RAPs installed at the project site, and 35-70 MN/m³ column stiffness values were measured that showed that the stiffness value used in the preliminary design (25 MN/m³) was on the safe side.

A full scale area load test was performed by a test embankment of 6.1 m height and 36.8 m x 36.8 m base dimensions, at an area where soil conditions were relatively more unfavorable and foundation layers were improved with RAP elements of 15 m length, installed in a square grid with 1.4 m spacing. Settlements were measured at 9 surface points, and a vibrating wire piezometer (transducers at 22.5 m and 27.5 m depths) and four inclinometers were installed at a depth of 40 m, which enabled the monitoring of pore pressures and lateral soil movements for a period of 52 days. The immediate settlements were observed to take place during the construction of the embankment, whereas the lower zone consolidation settlements were observed to continue at a decreasing rate. Settlements expected to occur under all structures when service loads are imposed were calculated by utilizing the estimated soil parameters from the back analysis of observed behavior at the field load test.

The construction of the wastewater treatment plant structures on soil layers improved with RAP elements was completed in about 6 months. During the water loading tests which were carried out to check the construction performance, settlement measurements were taken for up to 302 days. It was observed that under service loads, settlements reached were somewhat less than the estimated values based on test embankment observations; this was attributed to the differences in the extent of influence zones and the probable variation in soil conditions, as well as the rate of loading. The observed rate of settlements, indicating an almost final primary consolidation stage, were reached within the monitoring period in consistence with the predicted rates based on test embankment behavior.

The distribution of measured settlements on the plan has shown the differential settlements are considerably reduced by the implemented soil improvement and controlled to remain between 0.015% and 0.25% in accordance with the limiting values adopted among the project targets.

ACKNOWLEDGMENTS

This research was sponsored by Sentez Insaat, Istanbul, Turkey. The support of the company is greatly acknowledged. The authors also would like to acknowledge Akgirisim Muteahhitlik Musavirlik ve Cevre Teknolojileri San. ve Tic. A.S. for providing their valuable contributions and permission to publish the project data.

REFERENCES

ASTM D1143 – 81 (Reapproved 1994). *Standard test methods for deep foundations under static axial compressive load. Annual Book of ASTM Standards.*

Baez, J. J., and Martin, G. (1995). *Advances in the design of vibro systems for the improvement of liquefaction resistance.*

Brian, C. M., FitzPatrick, B. T., and Wissman, K. J. (2006). *Specifications for Impact® Rammed Aggregate Pier soil reinforcement*, Geopier® Foundation Company, Inc., Mooresville, NC.

Bowles, J. E. (1996). *Foundation analysis and design*, 5th Edition, The McGraw Hill Companies.

Das, B. M. (2014). *Principles of foundation engineering*, 8th Edition, Cengage Learning.

Farrell, T. M., Wallace, K., and Ho, J. (2010). "Liquefaction mitigation of three projects in California." *Proc. 5th International Conference Recent Advances in Geotechnical Earthquake Engineering and Soil Dynamics and Symposium in Honor of Professor I.M. Idriss*, San Diago, California.

Fox, S. N., and Edil, T. B. (2001). "Case histories rammed aggregate piers reinforcement construction over peat and highly organic soils." *Proc. Soft Ground Technology Conference*.



Handy, R. L. (2001). "Does lateral stress really influence settlement?" *ASCE Journal of Geotechnical and Geoenvironmental Engineering*, 623-626.

Lawton, E. C., and Fox, N. S. (1994). "Settlement of structures support on marginal or inadequate soils stiffened with short aggregate piers." *Proc., Vertical and Horizontal Deformations of Foundations and Embankments*, Geotechnical Special Publication No. 40, ASCE, College Station, Tex., Vol. 2, 962-974.

Lawton, E. C., Fox, N. S., and Handy, R. L. (1994). "Control of settlement and uplift structures using short aggregate piers." *Proc. ASCE National Convention*, Atlanta, Georgia, In-Situ Deep Soil Improvement, Geotechnical Special Publication No. 40, Atlanta, 121-132.

Meigh, A. C. (1987). *Cone penetration testing methods and interpretation*, CIRIA Ground Engineering Report: In-situ Testing. Latimer Trend & Company Ltd. Plymouth. Great Britain.

Poulos, H. G. (1993). *Settlement prediction for bored pile groups*, Deep Foundations on Bored and Auger Piles, Van Impe (ed.) © 1993 Balkema, Rotterdam.

Robertson, P. K., and Cabal, K. L. (2010). *Guide to cone penetration testing for geotechnical engineering*, 3rd Edition, Gregg Drilling & Testing, Inc., California, CPT Interpretation.

Robertson, P. K., and Cabal, K. L. (2010). "Estimating soil unit weight from CPT." *Proc. 2nd International Symposium on Cone Penetration Testing*, Huntington Beach, CA, USA.

Settle 3D Liquefaction Theory Manual © 2014 RocScience Inc.

Shamoto, Y., Zhang, J. M. and Tokimatsu, K. (1998). "New charts for predicting large residual post-liquefaction ground deformation." *Soil Dynamics and Earthquake Engineering*, 17, 427-438.

Sorensen, K. K. and Okkels, N. (2013). "Correlation between drained shear strength and plasticity index of undisturbed overconsolidated clays." *Proc. of the 18th International Conference on Soil Mechanics and Geotechnical Engineering*, Paris.

Wissmann, K. J., Moser, K., and Pando, M. (2001). "Reducing settlement risks in residual piedmont soil using rammed aggregate pier elements." *Proc., Foundations and Ground Improvement*, Geotechnical Special Publication No. 113, ASCE, Blacksburg, Va, 943-957.

Wissmann, K., FitzPatrick, B. T., White, D. J., and Lien, B. H. (2002). "Improving global stability and controlling settlement with geopier soil reinforcing elements." *Proc. 4th International Conference on Ground Improvement Techniques*, Kuala Lumpur, Malaysia.

Wissmann, K., Ballegooy, S. V., Metcalfe, B. C., Dismuke, J. N., and Anderson, C. K. (2015). "Rammed aggregate pier ground improvement as a liquefaction mitigation method in sandy and silty soils." *Proc. 6th International Conference on Earthquake Geotechnical Engineering*, Christchurch, New Zealand.

Zeng, W. (2010). *Assessment of matrix soil improvement using displacement aggregate piers*, Master of Science, Iowa State University, Ames, Iowa.



INTERNATIONAL JOURNAL OF
**GEOENGINEERING
CASE HISTORIES**

*The Journal's Open Access Mission is
generously supported by the following Organizations:*



Geosyntec
consultants

engineers | scientists | innovators

CONETEC



ENGEO
Expect Excellence

Access the content of the ISSMGE International Journal of Geoengineering Case Histories at:
<https://www.geocasehistoriesjournal.org>